Hindawi
Advances in Civil Engineering
Volume 2020, Article ID 8824414, 15 pages
https://doi.org/10.1155/2020/8824414

Research Article

Study of the Long-Term Deformation Characteristics of Municipal Sludge Solidified Soil under the Coupling Action of Dry-Wet Cycles and Initial Static Deviatoric Stress

Aiwu Yang,[1,2] Shaokun Yang,[1,2] Guofang Xu ,[3] and Wei Zhang[2]

[1]*College of Environmental Science and Engineering, Donghua University, Shanghai 201620, China*
[2]*Tianjin Key Laboratory of Soft Soil Characteristics and Engineering Environment, Tianjin 300384, China*
[3]*State Key Laboratory of Geomechanics and Geotechnical Engineering, Institute of Rock and Soil Mechanics, Chinese Academy of Sciences, Wuhan, Hubei 430071, China*

Correspondence should be addressed to Guofang Xu; gfxu@whrsm.ac.cn

Received 14 September 2020; Revised 9 October 2020; Accepted 23 October 2020; Published 11 November 2020

Academic Editor: Song-He Wang

A self-developed curing agent is used to solidify the municipal sludge taken from Tianjin. Then, the long-term deformation characteristics of the sludge solidified soil are investigated by means of unconsolidated undrained creep tests with different dry-wet cycles for considering the influence of climate. The experimental results show that the attenuation rate of the shear peak strength of municipal sludge solidified soil decreases gradually with the increase of the number of dry-wet cycles, and the strength remains unchanged when the number of dry-wet cycles is greater than 10. The variation laws under different initial static deviatoric stresses are basically identical. When the applied stress is less than the yield stress of the sludge solidified soil, the duration curves of creep show only attenuated stage, i.e., with very small deformation, and the deformation reaches a constant in a short period of time. When the deviatoric stress reaches the long-term strength of the soil, the instantaneous deformation of the sludge solidified soil becomes large and damage occurs quickly. Under the same deviatoric stress, the creep deformation increases with the increase of the number of dry-wet cycles. When the load applied in each step is of the same magnitude, the higher the initial static deviatoric stress is, the larger the deformation of sludge solidified soil will be. It is found that the stress-strain relationship and the relationship between creep strain and time can be well described by an exponential function and a hyperbolic function, respectively. On this basis, a creep model is proposed for the long-term deformation considering the effect of dry-wet cycle times and initial static deviatoric stress. The model is further validated by comparing the predictions with the test results under different deviatoric stresses; the good agreement between which shows the potential application of the model to relevant practical engineering.

1. Introduction

With the rapid development of economy and the acceleration of urbanization, municipal sludge treatment has become a hot issue that a great number of countries cannot avoid and needs to be solved urgently [1,2]. Sludge has high moisture content, poor mechanical properties and contains a large number of pathogens, microorganisms, heavy metals, and other harmful substances, which can cause serious secondary pollution and ecological problems if mishandled [3]. The traditional method of sludge treatment is inefficient and unsafe. The curing agent and skeleton materials are used to solidify municipal sludge, so that it can be recycled. After solidification, the physical and mechanical behaviors of the sludge are significantly improved, while the contents of organic matter and heavy metals are significantly reduced. Moreover, it is easier to be treated and transported than the original sludge, so that the municipal sludge can be transformed into the stable and safe subgrade filler for use to meet the engineering requirements and environmental requirements [4,5].

In recent years, many scholars have made great efforts and carried out a large number of experiments on the solidification of municipal sludge. By using different hybrid cement binders to add the sewage sludge with high organic content, Xin et al. [6] studied the unconfined compressive strength and leachability of heavy metals of sludge solidified soil. But when the cement is used to solidify sludge only, the strength of solidified body increases slowly, which is difficult to meet the requirements of resource utilization or landfill [7]. Qian et al. [8] investigated the potential for utilization of Municipal Solid Waste Incineration (MSWI) ash as solidification binder to treat heavy metals-bearing industrial waste sludge. The results showed that the matrixes with heavy metals-bearing sludge and MSWI ash have a strong fixing capacity for heavy metals: Zn, Pb, Cu, Ni, and Mn. Cerbo et al. [9] used the fly ash for solidification of heavy metal sludge and added several kinds of cement additives such as sodium sulfate, sodium carbonate, and ethylenediaminetetraacetic acid (EDTA) to the solidified matrix in order to ascertain its physical and chemical characterizations. Many other materials are also used with cement to solidify municipal sludge. In view of the shrinkage and cracking of cement solidified sludge, Wang et al. [10] added different proportions of cement, quicklime, and sand into sludge and found that the strength and stability of solidified soil are greatly improved. When heat treatment, chemical treatment, and physical treatment were performed on already solidified soil, it was found that the structure of the solidified soil was more stable [11]. However, when certain proportion of jarosite and alunite was added to cement solidified sludge soil, it was found that the incorporation of them had a significant reduction in soil strength, while the leaching content of heavy metals was significantly reduced [12]. Ballesteros et al. [13] investigated the solidification/stabilization of heavy metals in the electroplating sludge with the application of cement binder and admixtures of kaolinite clay, waste latex paint, and calcium chloride. Li et al. [14] found that adding an appropriate amount of waste glass powder was beneficial to the expansion of the sludge, which can make it possible to produce lightweight aggregates with high porosity and proper mechanical property.

On the other hand, the mechanical properties of soil under dry-wet cycles also arouse the interest of many investigators. Using γ-ray and X-ray tomography techniques, Pires et al. [15] and Wang et al. [16] found that the microstructures and the pore spatial distribution of soils were significantly altered under the dry-wet cycles, resulting in the changes of its macroscopic mechanical properties. For example, the shear strength and specific surface area of soil decreased significantly when the soil undergoes several dry-wet cycles [17,18]. In practical engineering, one can always meet the situation that many tensile cracks occur at the surface of mortar block stones covering the terrace soil in several years after the construction and instability and failure of the low-angle low-expansion soil slope. This can lead to the collapses of the soil slope and lots of fractures in the piles of foundation [19].

Likewise, sludge solidified soil, under natural environmental conditions, will be inevitably subjected to the dry-wet cycle caused by environmental and climate change [20,21]. Whether its mechanical properties can meet the engineering requirements needs to be further explored. The aforementioned scholars have made great progress in the preparation of urban sludge solidified soil and understanding its fundamental mechanical properties. However, there are few reports on the mechanical properties of municipal sludge solidified soil under the dry-wet cycle, and there is even a lack of experimental data on the long-term deformation during operation process. In view of this, in this paper, a series of triaxial creep tests were carried out on the sludge solidified soil under unconsolidated and undrained conditions, so as to explore its long-term deformation law under the coupling action of dry-wet cycle and initial static deviator stress. Then a model for reflecting the creep characteristics of solidified soil is proposed. The model can provide valuable information to the prediction of solidified soil deformation under long-term loading.

2. Testing Materials and Methods

2.1. Preparation of Solidified Earth Samples. The test adopts marine soft clay taken from Tianjin Binhai as the skeleton material, and its basic physical properties are shown in Table 1. The municipal sludge used in the test was taken from a sludge landfill in Tianjin, which was solid and had a strong and rancid smell. After being retrieved, the sludge was packed into plastic boxes for sealing and preservation under shade, and the temperature was kept at about 20°C. The municipal sludge used in the test was degradation. The basic physical properties of municipal sludge are shown in Table 2.

Due to the high moisture content of municipal sludge and the large amount of refractory organic matter, the direct curing treatment requires a large number of curing materials and has poor curing effect. The sludge is digested with quicklime before solidification, so as to reduce the moisture content and decompose organic matter. The specific content of quicklime added to municipal sludge needs to be tested. By referring to relevant literature, the quicklime content was designed to be 5%, 10%, 15%, 20%, 25%, and 30% of sludge quality. A certain amount of sludge and different amounts of quicklime were mixed and stirred evenly for the purpose of digestion test. After 24 hours' standing, the moisture content and organic matter content of sludge with different quicklime content were measured, respectively. The test results are shown in Figure 1.

It can be seen from Figure 1 that the quicklime has a significant effect on the digestion of sludge. In design range, the moisture content and the organic matter content in sludge declined with the increase of the content of quicklime. At the beginning, the decrease extent was obvious; then the curves became almost stable. For the water content, when the content of quicklime exceeds 15%, the decrease rate becomes stable. For organic matter content, the curve becomes a flat straight line when the lime content exceeds 20%. Considering the requirement of technology and economy, it is optimal when the quicklime content is 20%.

The curing agent used in the test is independently developed and this product has been applied for patents [22]. It

Table 1: Basic physical properties of coastal soft clay in Tianjin.

Void ratio	Water content (%)	Density (g/cm^3)	Specific gravity	Liquid limit (%)	Plastic limit (%)	Modulus of compression (MPa)
1.287	46.9	1.76	2.74	43.4	25.9	2.605

Table 2: Basic physical properties of municipal sludge.

Water content (%)	Organic matter (%)	Density (g/cm^3)	Specific gravity	pH
385.5	58.22	1.14	1.62	7.1

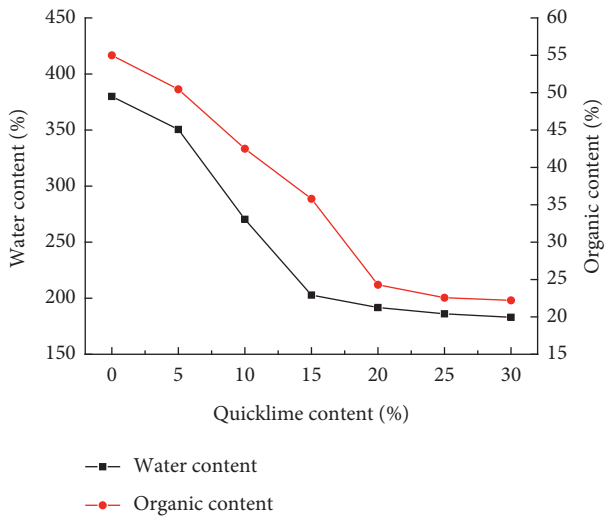

Figure 1: Effect of quicklime content on water content and organic matter content in municipal sludge.

is mainly composed of the main agent and the auxiliary agent of the curing agent. With the cement as the main agent, it plays a major role in the strength of sludge solidified soil. A small amount of auxiliaries A and B is added to catalyze the increase of strength growth rate and final strength. The toxicity of heavy metal leaching after curing meets the requirements of relevant specifications. The specific preparation scheme of municipal sludge solidified soil specimen is shown in Table 3.

2.2. The Manner of Dry-Wet Cycle. The sludge solidified soil samples prepared were put into the standard curing chamber for curing with 7, 14, 28, and 60 days, respectively. Then the basic physical properties of the samples after reaching the curing age and demoulding were tested. Table 4 shows the physical and mechanical properties of the solidified soil samples at the curing age of 28 days. It was found that the growth rate of unconfined compressive strength of the samples at the curing age of 28 days tended to be flat, which indicated that the internal reaction of soil mass was basically completed. Therefore, the wetting-drying tests were carried out on the samples at the curing age of 28 days.

The specific steps are as follows: first, put the samples with different times of dry-wet cycles into the oven to dry for 12 hours at low temperature (35 ± 3°C). Then, take out the samples and leave them at room temperature (20°C) for 1 to 2 hours. Wrap the samples with the plastic wrap and place them on the porous stone. Place the sample, along with the porous stone, into a custom mould (as shown in Figure 2), and fill the mould with water until the porous stone is submerged a little beyond the bottom of the sample. After standing, the samples would absorb water due to the capillary action of pores. When the upper surface of the soil samples is completely wet, the samples would be taken out and placed in an incubator at 20 ± 3°C for 24 hours. Finally, remove the film, clean the samples, and place them at room temperature for 1 hour. This is a dry-wet cycle process, which is shown in Figure 3. Repeat this operation until the specified number of times.

2.3. The Number of Dry-Wet Cycles. The relation curves between triaxial shear peak strength and the number of dry-wet cycles n under different initial static deviator stress q are shown in Figure 4.

As can be seen from Figure 4, with the increase of the number of dry-wet cycles, the peak strength of the sludge solidified soil generally showed a trend of significantly decreasing and then tending to be stable, and the variation law was basically identical under different levels of initial loads. It can be also seen that the peak intensity attenuates rapidly with the increase of the number of dry-wet cycles when $n \leq 5$, but the intensity attenuating rate gradually slows down. When $n = 5$, the attenuating amount accounts for more than 70% of the intensity attenuating amplitude. When n reaches 7 times, the curve flattens out. When n exceeds 10 times, the strength is basically stable and is no longer affected by the dry-wet cycle. This is mainly because the strength of sludge solidified soil mainly comes from the cementing substances produced by a series of hydration reactions between curing agent and soil particles and water. These cementing substances increase the bonding force between various particles and make the soil have a certain resistance to the dry-wet effects. After the first few times of dry-wet cycles, there are many cracks in the soil due to the dehydrated shrinkage and swelling of water absorption, which leads to a significant decrease in soil strength. However, after a certain number of dry-wet cycles, the intergranular bonding force and the stress generated by dry-wet cycles gradually tend to balance and reach a steady state. So, the cracks no longer continue to expand, and the strength gradually becomes stable. This indicates that the shear resistance of soil decreases with the

Table 3: Preparation scheme of municipal sludge solidified soil.

Solidifying material	Sludge-to-dry soil ratio	Quicklime	Water	Main curing agent	Auxiliary curing agent A	Auxiliary curing agent B
Content (%)	1 : 3	20	40	10	0.6	0.3

Note: the quality of quicklime is added according to the percentage of sludge quality. The quality of main curing agent, auxiliary curing agent, and water are added according to the percentage of total mass of sludge and dry soil.

Table 4: Basic physical properties of sludge solidified soil.

Water content (%)	Density (g/cm^3)	Dry density (g/cm^3)	Unconfined compressive strength (kPa)	pH
33.4	1.59	1.19	365.3	8.6

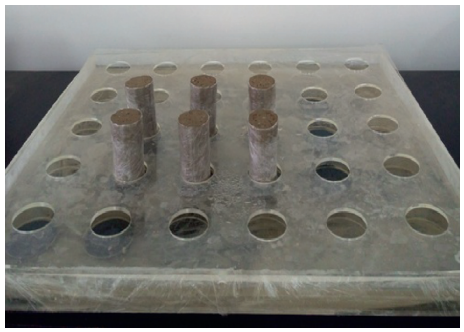

Figure 2: Slaking test mould.

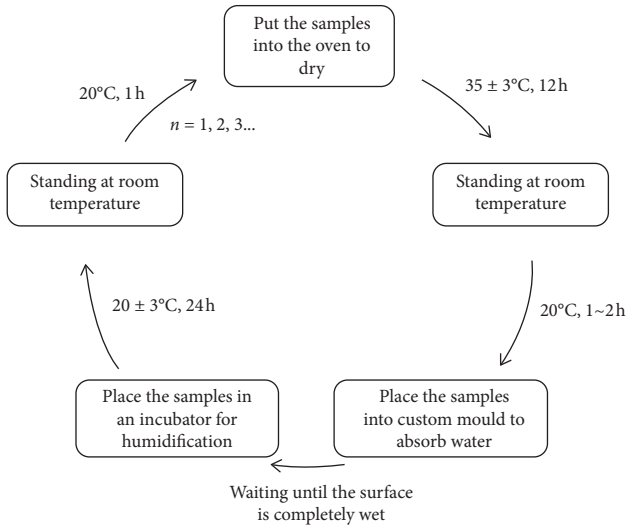

Figure 3: Flowchart of dry-wet cycles.

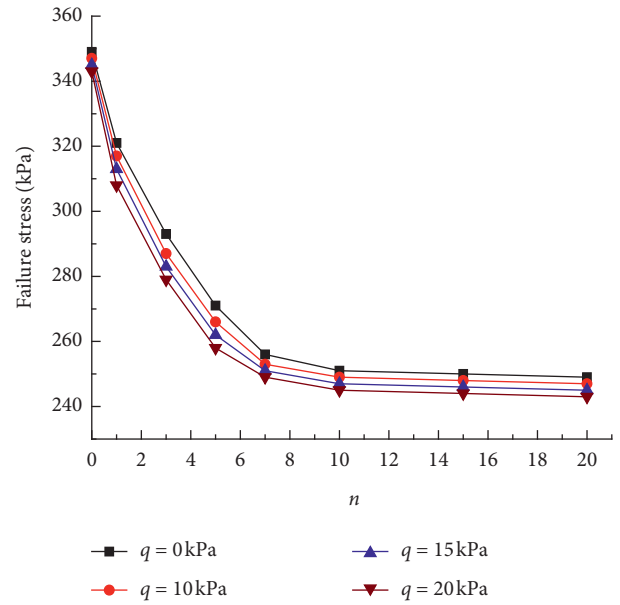

Figure 4: Relationship between peak strength of triaxial shear and dry-wet cycles.

increase of the number of dry-wet cycles. When a certain number of dry-wet cycles is reached, the influence of dry-wet cycles on the triaxial shear strength is no longer significant.

According to the above analysis, it is reasonable to choose 0, 1, 3, 5, 7, and 10 times as the dry-wet cycles.

3. Testing Scheme

In order to research the long-term performance of municipal sludge solidified soil, TSS10 triaxial rheological test instrument was used to conduct creep test under unconsolidated and undrained conditions, so as to simulate the engineering situation with poor drainage conditions in the actual site. Considering that the subgrade soil has certain buried depth and will be subjected to additional static stress of the upper soil, the initial static deviator stress q of 0, 10, 15, and 20 kPa was selected for the study.

At present, there are two loading methods of creep test: graded loading and separate loading. The latter is to test a number of identical soil samples, while the former is to apply various levels of stress step by step on the same soil samples. In order to eliminate the influence of the differences between samples on the test results, the creep tests were carried out by means of graded loading. The creep loading was determined by the conventional triaxial shear test (UU), and the confining pressure σ_3 was chosen to be 20 kPa to simulate the condition of small fill thickness. Let $s = (\sigma_1 - \sigma_3)$ represent the deviator stress. The creep test loading series is usually 5–8 groups, and then the increment of stress level of each class is calculated. As for the determination of creep stability criteria, there is no clear specification yet. In this paper, if the axial strain ε was less than 0.01 mm within 48 hours,

the next stress level test would be conducted. The specific test scheme was shown in Table 5.

4. Creep Property

According to the available test results, the complete strain and time curves at each level of stress cannot be obtained directly. The curves are step-like and cannot be directly applied to analysis and research. Instead, the superposition numerical method is needed to transform them into curves under separate loading. In this paper, "Chen's method" [23] is used to establish the superposition relationship in the real deformation process.

4.1. Creep Testing Curve. The creep duration curves of the sludge solidified soil under the action of different numbers of dry-wet cycle and initial static bias stress are shown in Figure 5.

It can be seen from Figure 5 that when the deviant stress is less than the yield stress, the creep curves of sludge solidified soil under different numbers of dry-wet cycles all present attenuation type of creep morphology. The overall trend of the duration curves under all steps is similar, which shows that the deformation amount is relatively small and tends to be stable within the deformation time. As time progresses, the strain growth rate slows down and eventually tends to a certain stable value. And the greater the deviator stress is, the longer it takes to reach the stable value. Under the action of the last step, the curve grows approximately linearly, which indicates that the deviator stress level has reached the long-term strength of soil, and the soil has a large instantaneous deformation after being acted on by external forces, resulting in a large deformation and rapid failure at the initial stage.

It can also be seen from Figure 5 that when the load applied in each step is of the same magnitude, the higher the initial static deviatoric stress is, the larger the deformation of sludge solidified soil will be. When the deviator stress levels are the same, the soil deformation at stability increases with the increase of the number of dry-wet cycles. This is because the soil structure disturbance increases with the increase of dry-wet cycles. Its internal connection becomes looser because of the increase of soil structure damage. Consequently, its stability and ability to resist external deformation are weakened. With the increase of stress level, creep deformation increases rapidly when the deviatoric stress exceeds the long-term strength of soil.

4.2. Creep Model of Sludge Solidified Soil

4.2.1. Establishment of Creep Model. According to the creep curves in Figure 5, the strain of the solidified soil shows certain attenuation characteristics. There are many kinds of creep models. The models with few and easy-to-get parameters have some advantages. Exponential function, logarithmic function, power function, and hyperbolic function were used to fit the strain-time relation curves, respectively, with the least square method. The results show that the initial strain value is higher and the final settlement value is lower when the exponential function is used for fitting. By using logarithmic function and power function fitting, the strain grows slowly and continuously. It is worth noting that the strain increases rapidly in the later period and deviates from the test curve, while the hyperbolic relation is more practical [24].

Table 5: Testing scheme.

n	q (kPa)	s (kPa)	t (h)	σ_3 (kPa)
0, 1, 3, 5, 7, 10	0, 10, 15, 20	50⟶100⟶150⟶⋯⟶ (damage)	96	20

According to the above analysis, the stress-strain relationship is the relation between the strain and the deviator stress $(\sigma_1 - \sigma_3)$, the number of dry-wet cycles n, and the initial static deviator stress q. The stress-strain relation curve is tentatively expressed by the function $f((\sigma_1 - \sigma_3), n, q)$, while the strain-time relation curve is expressed by the hyperbolic function. Therefore, the creep expression is assumed as shown in the following equation:

$$\varepsilon = f\left((\sigma_1 - \sigma_3), n, q\right) \times \frac{t}{At + B}. \tag{1}$$

Command $B/A = C$. And C is also a function of the number of dry-wet cycles n, initial static bias stress q, and deviator stress $(\sigma_1 - \sigma_3)$. Transform equation (1) to

$$\varepsilon = \frac{1}{A} \times f\left((\sigma_1 - \sigma_3), n, q\right) \times \frac{t}{t + C} = F \times \frac{t}{t + C}, \tag{2}$$

where F is equal to $(1/A) \times f((\sigma_1 - \sigma_3), n, q)$. It is still a function of the number of dry-wet cycles n, initial static bias stress q, and deviator stress $(\sigma_1 - \sigma_3)$.

4.2.2. Determination of Creep Model Parameters. For the municipal sludge solidified soil studied, when the number of dry-wet cycles, initial static deviator stress and stress level are determined, the function F is a constant F_0, which can be expressed as

$$\varepsilon = F_0 \times \frac{t}{t + C}. \tag{3}$$

Transform equation (3) to get

$$\frac{t}{\varepsilon} = \frac{t + C}{F_0}. \tag{4}$$

On the basis of equation (4), the creep curves can be transformed into the $t/\varepsilon - t$ curves, and then linear fitting can be used to obtain the parameter values C_1 and C_2 taking into account the influence of different dry-wet cycles n and different initial static deviator stress q, respectively.

In order to explore the influence of dry-wet cycles on the long-term deformation of sludge solidified soil, the creep curves of initial static bias stress $q = 0$ kPa were selected as the research object. Figure 6 shows the $t/\varepsilon - t$ relationship curves under different numbers of dry-wet cycles.

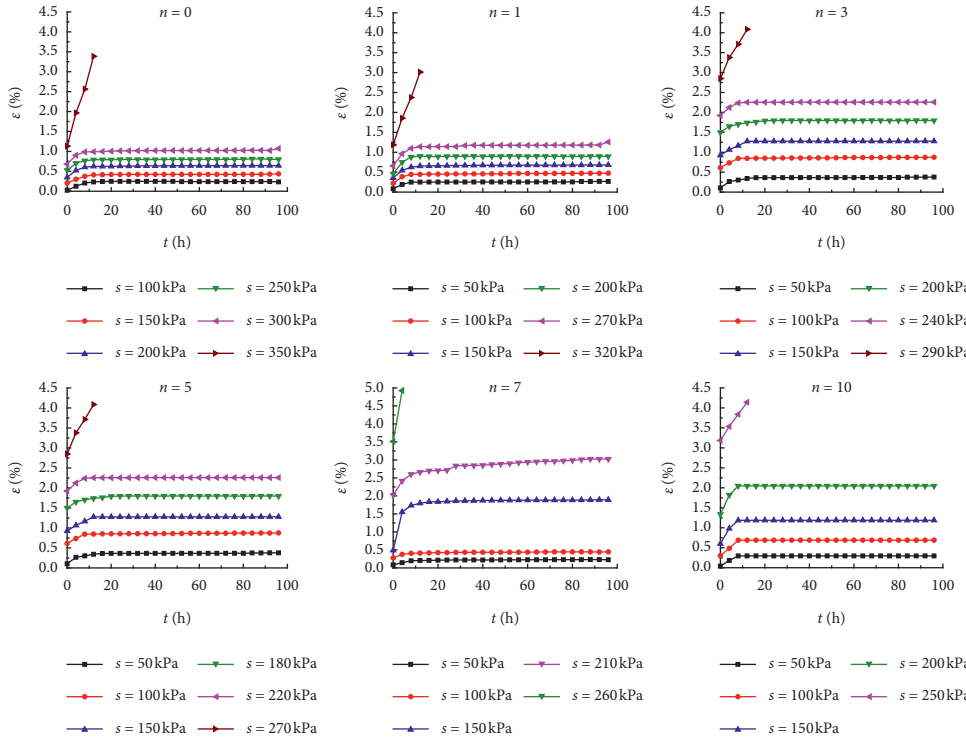

(a)

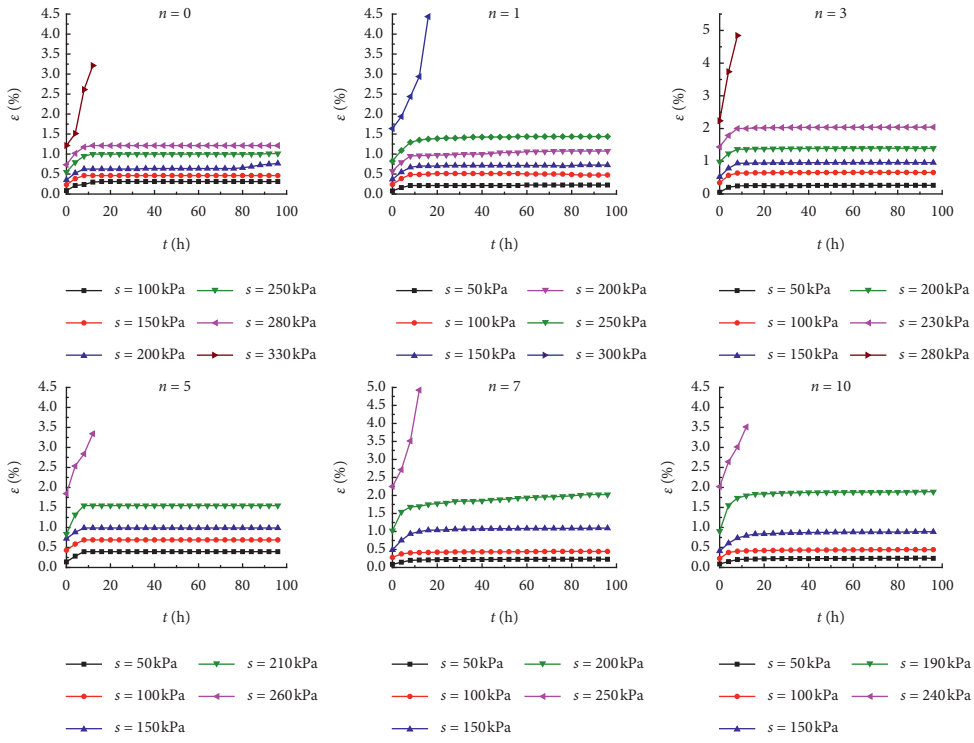

(b)

Figure 5: Continued.

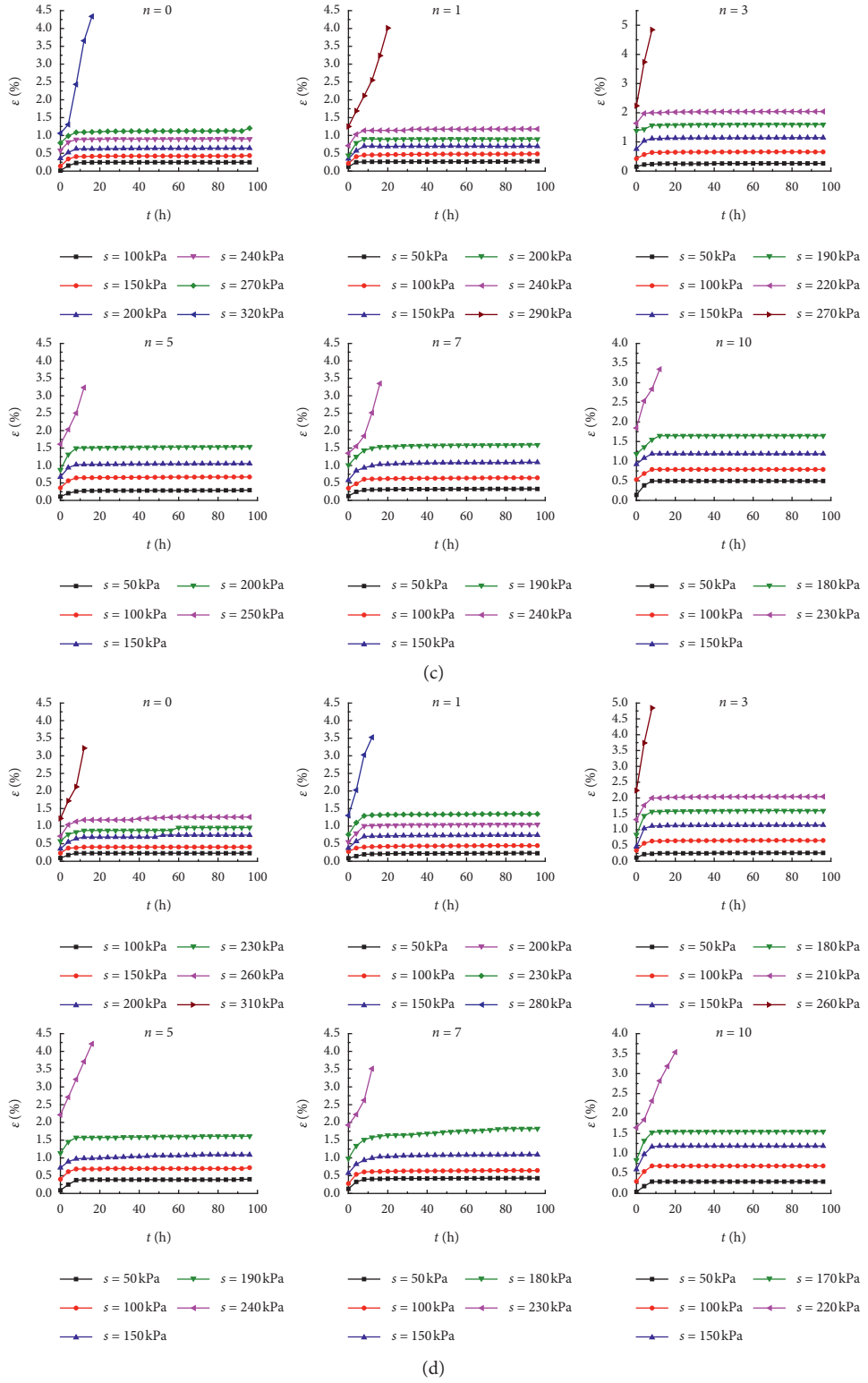

Figure 5: Duration curves of creep. (a) $q = 0$ kPa, (b) $q = 10$ kPa, (c) $q = 15$ kPa, and (d) $q = 20$ kPa.

It can be seen from Figure 5 that the linear fitting of the $t/\varepsilon - t$ relation curves get better effects, and the fitting degree R^2 can reach more than 90%. The intercept a_1 and slope b_1 of each fitting curve on the t/ε-axis are shown in Table 6.

As shown in Table 6, under the same initial static deviator stress, when the number of dry-wet cycles is constant, the parameter C_1 does not change much at each stress level. That is, the magnitude of deviator stress has little influence on the value of parameter C_1. And the average value of

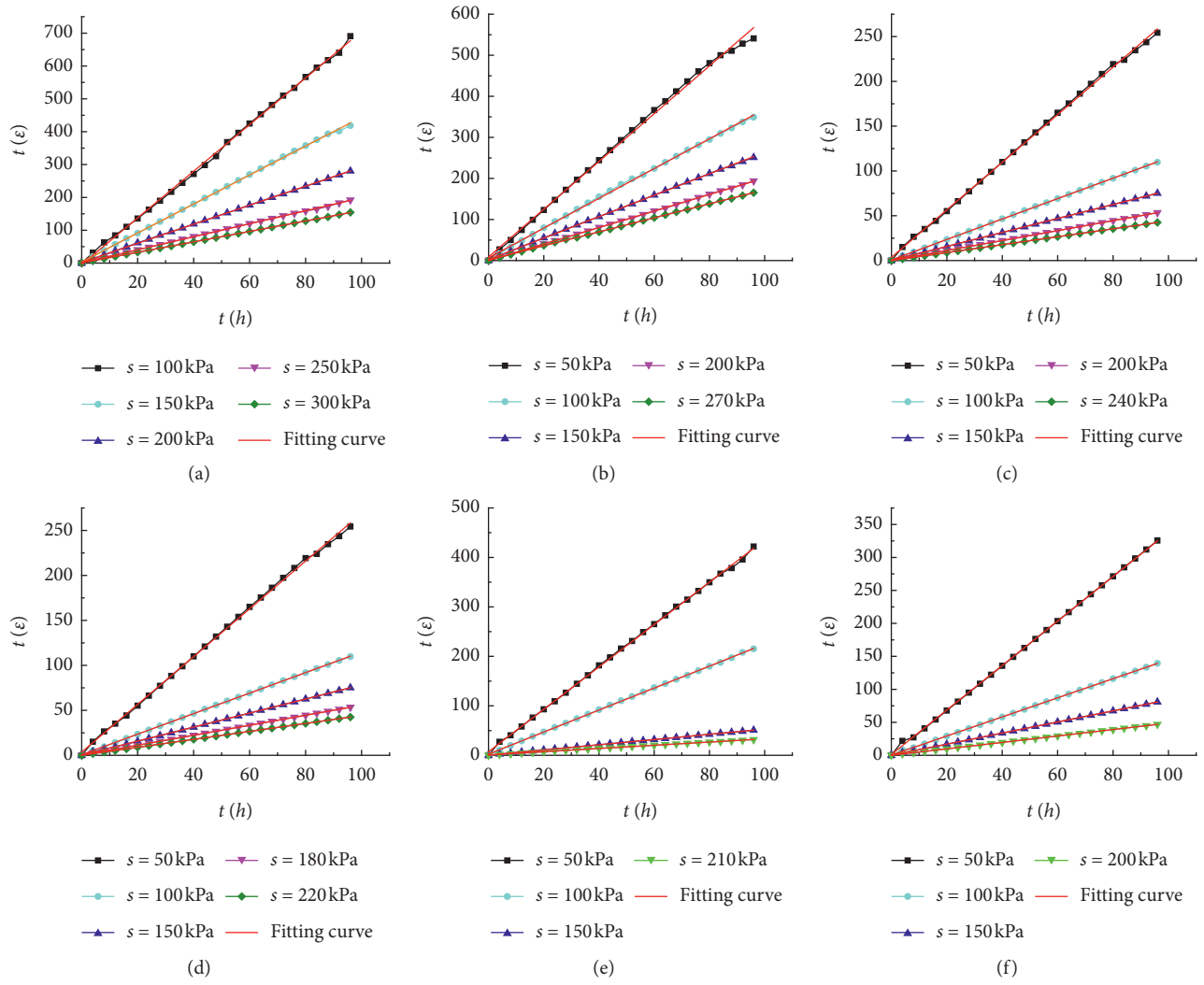

Figure 6: Curves between t/ε and t under different numbers of dry-wet cycles. (a) $n = 0$, (b) $n = 1$, (c) $n = 3$, (d) $n = 5$, (e) $n = 7$, and (f) $n = 10$.

parameter C_1 under different dry-wet cycles also changes little, so the final average value of parameter C_1 is set as 0.6478.

When $t = 96$ h, the creep variable ε was taken to calculate the F_0 corresponding to different numbers of dry-wet cycles. Since F is the function of the number of dry-wet cycles n, the initial static deviator stress q, and the deviator stress $(\sigma_1 - \sigma_3)$, when the initial static deviator stress and the number of dry-wet cycles are constant, F becomes a function of the deviator stress. The exponential function $y = ab^x$ is used to describe the relationship between F and the deviator stress level. The results are shown in Figure 7.

As shown in Figure 7, the exponential function can be used to describe the change relationship between F and $(\sigma_1 - \sigma_3)$, with both R^2 reaching more than 95%. The parameter values of a_1 and b_1 are shown in Table 7.

Table 7 shows that parameters a_1 and b_1 change to different degrees with the increase of the number of dry-wet cycles. Therefore, the relationship between parameters a_1 and b_1 and the number of dry-wet cycles n is further studied, which is as shown in Figure 8.

Figure 8 shows that it is suitable to use power function and linear function, respectively, to describe the relationship between parameters a_1 and b_1 and the number of dry-wet cycles n. And the fitting degree R^2 all can reach more than 96%. The specific expressions are shown in the following equations:

$$a_1 = 0.09638 \times (1 + n)^{0.59213}, \tag{5}$$

$$b_1 = 1.00543 + 7.62103 \times 10^{-4} \times n. \tag{6}$$

In order to discuss the influence of initial static deviatoric stress on the long-term deformation of sludge solidified soil, the creep curves of sludge solidified soil under different initial static deviating stresses at $n = 3$ were randomly selected as the research object. The creep curves were also transformed into the $t/\varepsilon - t$ curves and fitted linearly, as shown in Figure 9. The parameter values are shown in Table 8.

Similarly, it can be seen from Table 8 that under the same dry-wet cycles, when the initial static deviator stress is

Table 6: Parameter values under different numbers of dry-wet cycle when q is equal to 0.

n	s (kPa)	Intercept a_1	Slope b_1	Parameter C_1	Average value of C_1
0	100	4.3069	7.0973	0.6068	0.6314
	150	3.5168	5.4074	0.6504	
	200	2.4121	3.8984	0.6187	
	250	1.9690	2.9772	0.6614	
	300	0.9862	1.5920	0.6195	
1	50	3.9127	5.8147	0.6729	0.6707
	100	2.5331	3.6233	0.6991	
	150	2.4866	2.6103	0.6526	
	200	1.7572	2.5431	0.6910	
	270	0.7148	1.1205	0.6379	
3	50	2.4568	3.6548	0.6722	0.6338
	100	0.7065	1.1406	0.6194	
	150	0.4329	0.7127	0.6074	
	200	0.3097	0.5135	0.6031	
	240	0.2951	0.4425	0.6669	
5	50	2.5567	3.6548	0.6995	0.6546
	100	0.7981	1.1406	0.6997	
	150	0.4871	0.7798	0.6246	
	180	0.3397	0.5550	0.6120	
	220	0.2895	0.4542	0.6373	
7	50	3.2465	4.8349	0.6715	0.6601
	100	1.4568	2.2234	0.6552	
	150	0.6913	1.0990	0.6291	
	210	0.2235	0.3265	0.6845	
10	50	1.8112	2.7379	0.6615	0.6361
	100	0.8765	1.4472	0.6057	
	150	0.5432	0.8410	0.6459	
	200	0.3464	0.5488	0.6312	

constant, the parameter C_2 does not change much at each stress level. That is, the magnitude of deviator stress has little influence on the value of parameter C_2. And the average value of parameter C_2 under different initial static deviator stress also changes little, so the final average value of parameter C_2 is set as 0.5716.

When $t = 96$ h, the creep variable ε was taken to calculate F_0 corresponding to different initial static deviator stress. Since F is the function of the number of dry-wet cycles n, the initial static deviator stress q, and the deviator stress $(\sigma_1 - \sigma_3)$, when the initial static deviator stress and the number of dry-wet cycle are constant, F becomes a function of the deviator stress. The exponential function $y = ab^x$ is the same used to describe the relationship between F and the deviator stress level. The results are shown in Figure 10.

As shown in Figure 10, the exponential function can be used to describe the change relationship between F and $(\sigma_1 - \sigma_3)$, with both R^2 reaching more than 95%. The parameter values of a_2 and b_2 are shown in Table 9.

Table 9 shows that parameters a_2 and b_2 change to different degrees with the increase of the initial static deviator stress q. The relationship between parameters a_2 and b_2 and q is as shown in Figure 11.

Figure 11 shows that it is suitable to use power function and linear function, respectively, to describe the relationship between parameters a_2 and b_2 and the initial static deviatoric stress q. The specific expressions are shown in the following equations:

$$a_2 = 0.20651 + 0.18535 \times 0.8536^q, \tag{7}$$

$$b_2 = 1.00766 + 1.59029 \times 10^{-4} \times q. \tag{8}$$

In the above analysis process, F is the function of the number of dry-wet cycles n, initial static bias stress q, and deviator stress $(\sigma_1 - \sigma_3)$. Therefore, when considering the influence of the dry-wet cycles, the initial static deviator stress is assumed to be a certain value, and then the relationship between F and the deviator stress level is analyzed. By using the exponential function $y = ab^x$ to fit the data values, the functional relationship between the values of a_1 and b_1 and the numbers of dry-wet cycles could be obtained. In the same way, when the influence of initial static deviator stress is taken into account, it assumes that the number of dry-wet cycles is a certain value. By using the exponential function $y = ab^x$ to fit the data values, the functional relationship between the values of a_2 and b_2 and the initial static deviator stress, the fitting results show that the number of dry-wet cycles and the initial static deviator stress all have influences on parameters a and b. Just the influence degree of impact varies. So, it can be considered that the parameters a and b are functions of the number of dry-wet cycles and initial static deviator stress, but the idea of single variable method is adopted in the analysis process. In the actual research process, when considering the influence of the dry-wet cycles, the initial static deflection stress is randomly selected. And when considering the influence of initial static deviator stress, the number of dry-wet cycles is also arbitrarily selected. Therefore, it can be

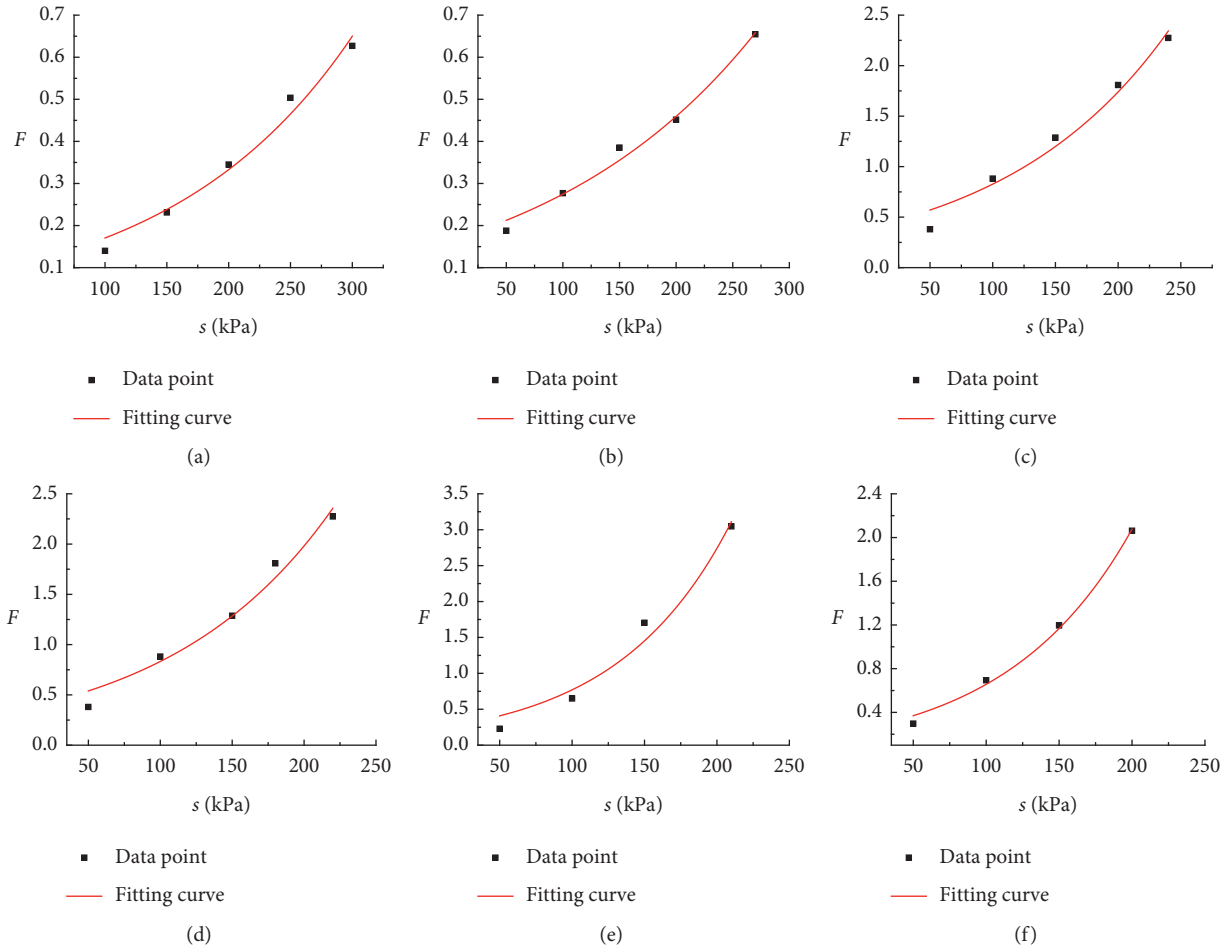

Figure 7: Relationship between F and deviatoric stress under different dry-wet cycles when q is equal to 0. (a) $n = 0$, (b) $n = 1$, (c) $n = 3$, (d) $n = 5$, (e) $n = 7$, and (f) $n = 10$.

Table 7: Parameter values of a_1 and b_1.

n	0	1	3	5	7	10
a_1	0.0873	0.1642	0.2078	0.2166	0.3497	0.3929
b_1	1.0052	1.0067	1.0075	1.0087	1.0116	1.0128

approximately assumed that the functions of parameters a and b on the number of dry-wet cycles and the initial static deflection stress are the same function. On this basis, by the synthesis of equations (5)–(8), functions of a and b on the number of dry-wet cycles and initial static deviator stress are obtained as shown in the following equations:

$$a = \frac{(\alpha_1 + \beta_1 \times k_1^q)^2}{\alpha_2 \times (1+n)^{\beta_2}}, \tag{9}$$

$$b = \frac{(\alpha_3 + \beta_3 \times n)^2}{\alpha_4 + \beta_4 \times q}. \tag{10}$$

According to the above analysis results, the influence of deviator stress, dry-wet cycles, and initial static deviator stress on parameter C can be ignored. The parameter C can be approximately taken as the average value of C_1 and C_2, which is equal to 0.6097.

To sum up, equations (9) and (10) are substituted into equation (2) to obtain the prediction formula of long-term deformation of sludge solidified soil under the action of different number of dry-wet cycles and initial static biased stresses. The results are shown as follows:

$$\varepsilon = \frac{(\alpha_1 + \beta_1 \times k_1^q)^2}{\alpha_2 \times (1+n)^{\beta_2}} \times \left[\frac{(\alpha_3 + \beta_3 \times n)^2}{\alpha_4 + \beta_4 \times q}\right]^{(\sigma_1 - \sigma_3)} \times \frac{t}{t + C}, \tag{11}$$

where q represents the initial static bias stress, n is the number of dry-wet cycles, t represents time, and $(\sigma_1 - \sigma_3)$ is the deviator stress. The values of other parameter in the equation are shown in Table 10.

4.2.3. Verification of the Creep Model. In order to verify the accuracy and applicability of the creep prediction formula,

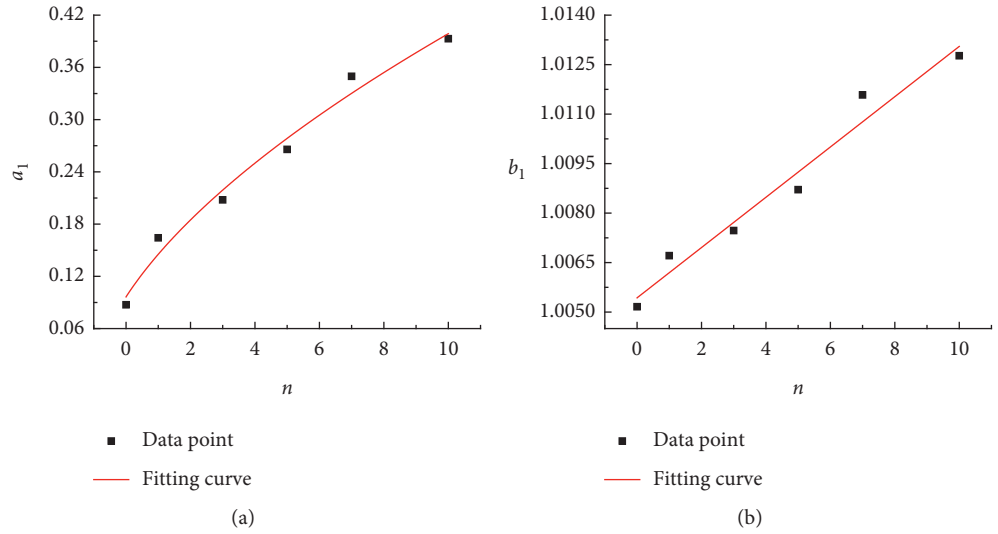

Figure 8: Relationship curves between parameters of a_1 and b_1 and numbers of dry-wet cycle. (a) a_1 and (b) b_1.

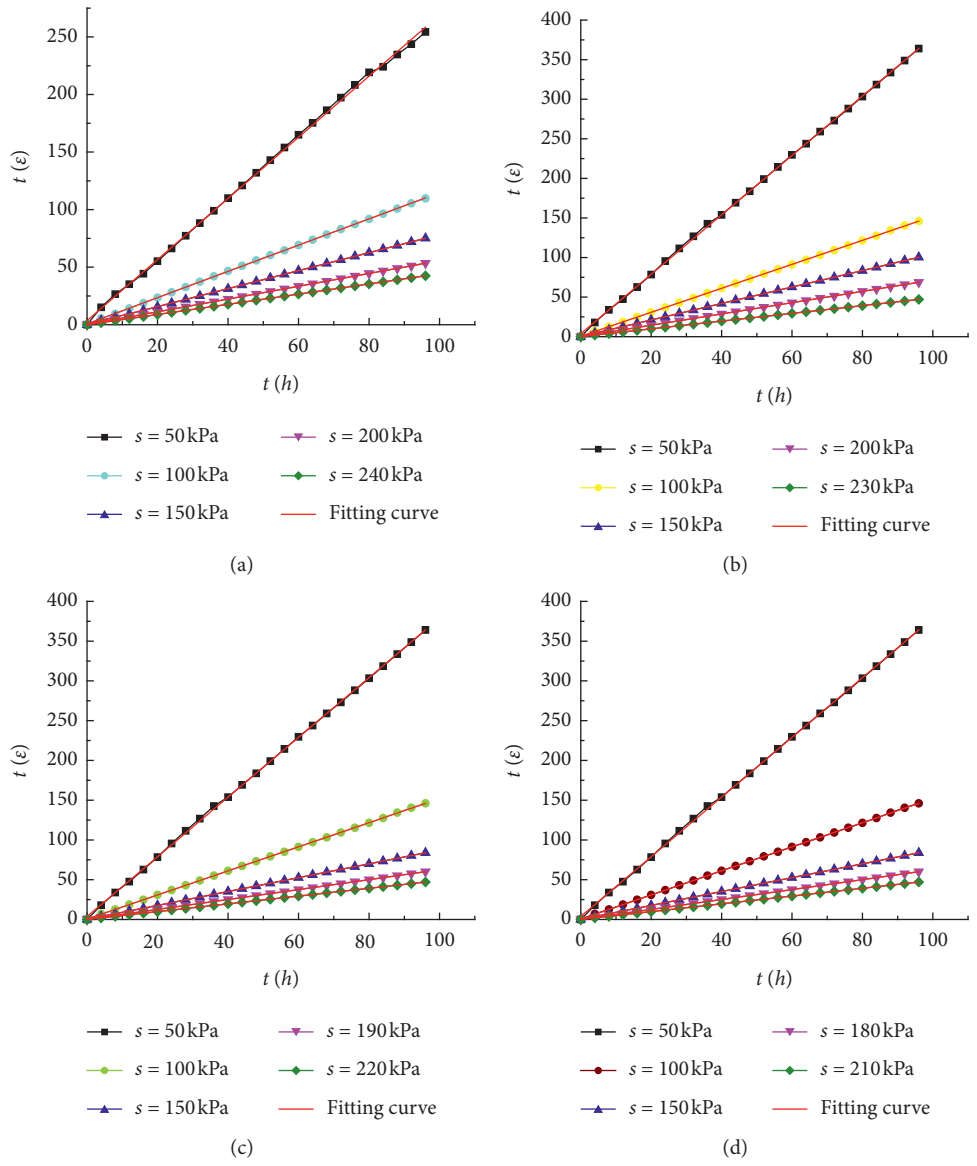

Figure 9: Curves between t/ε and t under different initial static deviator stress. (a) $q = 0$ kPa, (b) $q = 10$ kPa, (c) $q = 15$ kPa, and (d) $q = 20$ kPa.

Table 8: Parameters of $n = 3$ under different initial static deviatoric stress.

q (kPa)	s (kPa)	Intercept a_2	Slope b_2	Parameter C_2	Average value of C_2
0	50	2.4568	3.6548	0.6722	0.6338
	100	0.7065	1.1406	0.6194	
	150	0.4329	0.7127	0.6074	
	200	0.3097	0.5135	0.6031	
	240	0.2951	0.4425	0.6669	
10	50	2.5676	4.7539	0.5401	0.5256
	100	0.7650	1.5149	0.5050	
	150	0.5432	1.0416	0.5215	
	200	0.4322	0.8131	0.5315	
	230	0.2599	0.4904	0.5300	
15	50	2.2349	3.7539	0.5953	0.5638
	100	0.8505	1.5049	0.5651	
	150	0.4602	0.8713	0.5282	
	190	0.3437	0.6241	0.5507	
	220	0.2838	0.4893	0.5799	
20	50	3.8279	3.8279	0.5838	0.5630
	100	0.8950	1.6515	0.5419	
	150	0.4826	0.8098	0.5959	
	180	0.3144	0.5662	0.5552	
	210	0.2632	0.4890	0.5382	

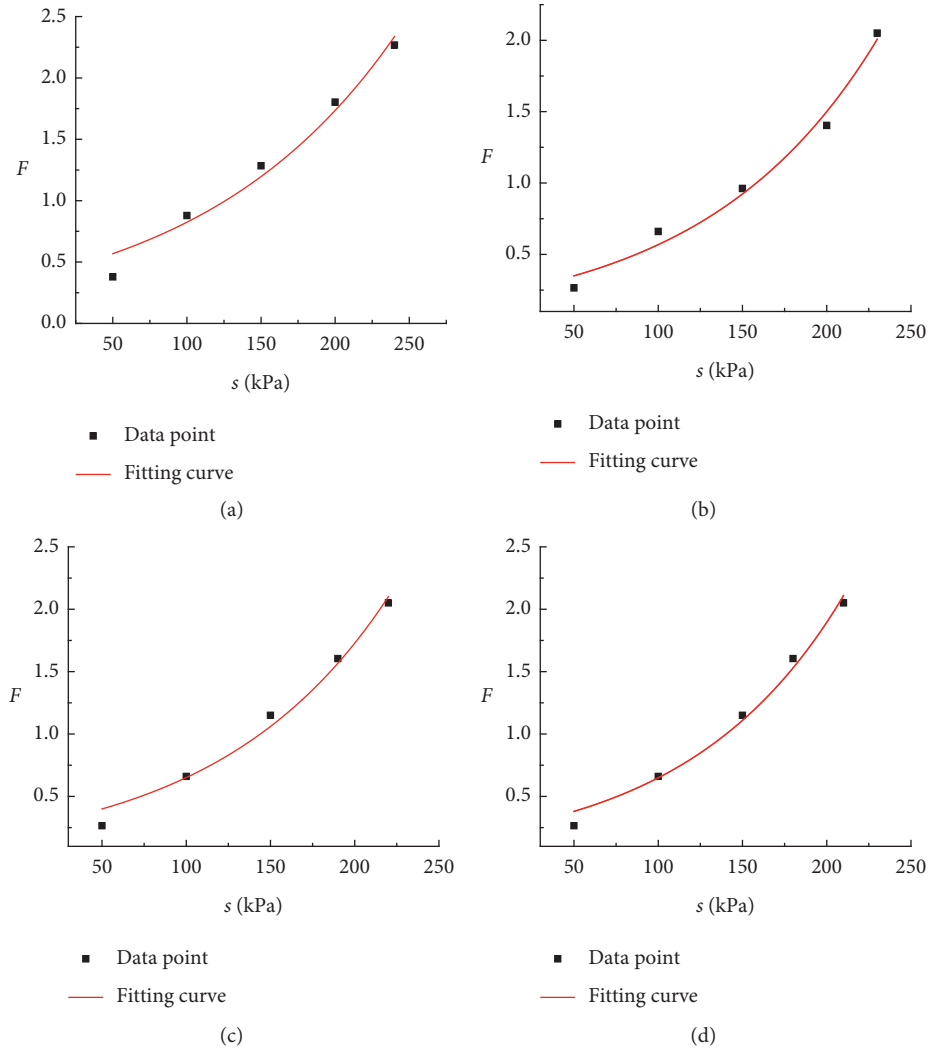

Figure 10: Relationship between F and deviatoric stress under different initial static deviatoric stresses. (a) $q = 0$ kPa, (b) $q = 10$ kPa, (c) $q = 15$ kPa, and (d) $q = 20$ kPa.

Table 9: Parameter values of a_2 and b_2.

q (kPa)	0	10	15	20
a_2	0.39183	0.2452	0.22235	0.21515
b_2	1.00747	1.00976	1.00981	1.01077

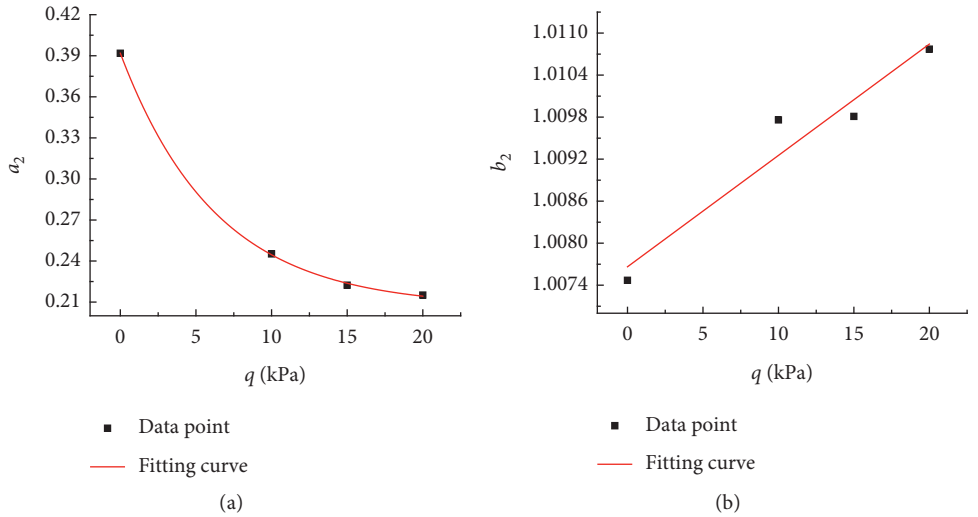

Figure 11: Relationship curves between parameters of a_2 and b_2 and initial static deviatoric stress. (a) a_2 and (b) b_2.

Table 10: Specific parameter values of equation (11).

α_1	β_1	k_1	α_2	β_2	α_3	β_3	α_4	β_4	C
0.20551	0.18535	0.8536	0.09638	0.59213	1.00543	$7.62103*10^{-4}$	1.00766	$1.59029*10^{-4}$	0.6097

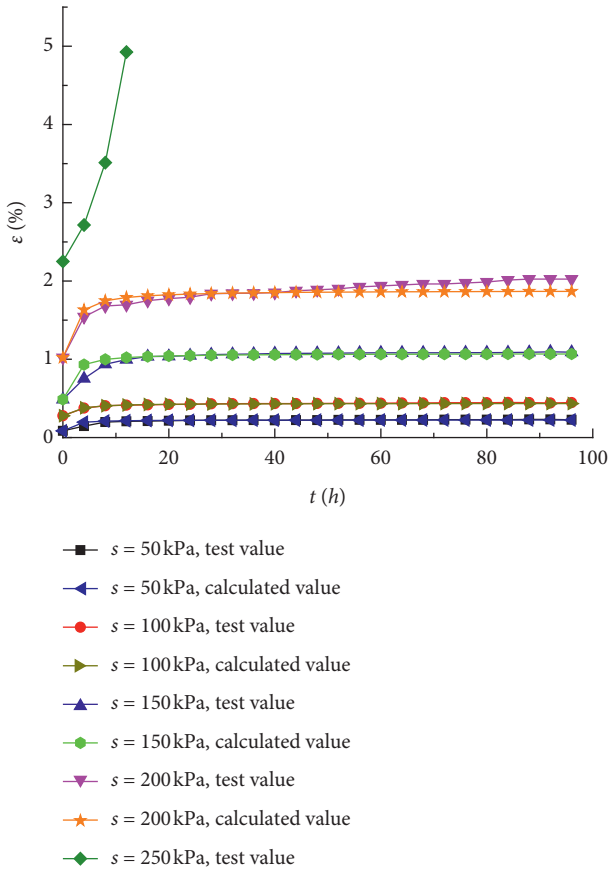

Figure 12: Contrast figures between calculated values and experimental values.

the experimental values under different initial static deviating stresses and different numbers of dry-wet cycles were compared with the creep values calculated by equation (11). Take the initial static bias stress $q = 10$ kPa and the number of dry-wet cycles $n = 7$ as an example. The predicted results are shown in Figure 12.

Figure 12 shows that the calculated creep value is close to the experimental data. And the overall variation trend of the two curves is basically the same, which indicates that the prediction formula can meet the requirements of strain variation with time.

5. Conclusions

A series of creep tests were carried out on the sludge solidified soil under the condition of unconsolidated and undrained. Then the characteristic of long-term deformation of the soil under coupling action of dry-wet cycle and initial static deviator stress was discussed. The key conclusions are as follows:

(1) The attenuation rate of the shear peak strength of municipal sludge solidified soil decreases gradually with the increase of the number of dry-wet cycles, and the strength remains unchanged when the number of dry-wet cycles is greater than 10. The variation laws under different initial static deviatoric stresses are basically identical. After the first few times of dry-wet cycles, there are many cracks in the soil due to the dehydrated shrinkage and swelling of water absorption, which leads to a significant decrease in soil strength. However, after a certain number of dry-wet cycles, the intergranular bonding force and the stress generated by dry-wet cycles gradually tend to balance and reach a steady state. So, the cracks no longer continue to expand, and the strength gradually becomes stable.

(2) When the applied stress is less than the yield stress of the sludge solidified soil, the duration curves of creep show only attenuated stage. The development rate of strain slows down and quickly enters the stable stage. When the deviatoric stress reaches the long-term strength of soil, the instantaneous deformation of the sludge solidified soil becomes large and damage occurs quickly. When the load applied in each step is of the same magnitude, the higher the initial static deviatoric stress is, the larger the deformation will be. Under the identical condition of deviator stress, the creep variable increases with the increase of the number of dry-wet cycles.

(3) Based on the hyperbolic strain-time relationship and stress-strain index function relation, the influence of the number of dry-wet cycles and the initial static stress on the deformation was analyzed by using the single-variable method. On this basis, a creep model is proposed for the long-term deformation considering the effect of dry-wet cycle times and initial static deviatoric stress. The model can provide theoretical support for the prediction of deformation of solidified soil under long-term loading.

Data Availability

Some or all data used to support the findings of this study are available from the corresponding author upon request (E-mail: gfxu@whrsm.ac.cn).

Conflicts of Interest

The authors declare that there are no conflicts of interest regarding the publication of this paper.

Acknowledgments

Financial support from the National Natural Science Foundation of China (Grant no. 51978440) and Tianjin Science and Technology Project (Grant nos. 19JCZDJC39700 and 2016CJ01) is greatly acknowledged.

References

[1] Y. N. Chun, M. S. Lim, and K. Yoshikawa, "Characteristics of the product from steam activation of sewage sludge," *Journal of Industrial and Engineering Chemistry*, vol. 18, no. 2, pp. 839–847, 2012.

[2] A. Grönroos, H. Kyllönen, K. Korpijärvi et al., "Ultrasound assisted method to increase soluble chemical oxygen demand (SCOD) of sewage sludge for digestion," *Ultrasonics Sonochemistry*, vol. 12, no. 1-2, pp. 115–120, 2005.

[3] R. F. Vieira, W. Moriconi, and R. A. A. Pazianotto, "Residual and cumulative effects of soil application of sewage sludge on corn productivity," *Environmental Science and Pollution Research*, vol. 21, no. 10, pp. 6472–6481, 2014.

[4] J. M. Reid and A. H. Brookes, "Investigation of lime stabilised contaminated material," *Engineering Geology*, vol. 53, no. 2, pp. 217–231, 1999.

[5] G. Zhen, X. Lu, X. Cheng, H. Chen, X. Yan, and Y. Zhao, "Hydration process of the aluminate $12CaO{\cdot}7Al_2O_3$-assisted Portland cement-based solidification/stabilization of sewage sludge," *Construction and Building Materials*, vol. 30, pp. 675–681, 2012.

[6] D. Xin, X. Chai, and W. Zhao, "Hybrid cement-assisted dewatering, solidification and stabilization of sewage sludge with high organic content," *Journal of Material Cycles and Waste Management*, vol. 18, no. 2, pp. 356–365, 2016.

[7] X. Sun, W. Zhu, X. Qian, and Z. Xu, "Exploring cementitious additives for pretreatment of high-early-strength sewage sludge from the perspective of the rapid generation of non-evaporable water," *Journal of Materials in Civil Engineering*, vol. 26, no. 5, pp. 878–885, 2014.

[8] G. Qian, Y. Cao, P. Chui, and J. Tay, "Utilization of MSWI fly ash for stabilization/solidification of industrial waste sludge," *Journal of Hazardous Materials*, vol. 129, no. 1-3, pp. 274–281, 2006.

[9] A. A. V. Cerbo, F. Ballesteros, T. C. Chen, and M.-C. Lu, "Solidification/stabilization of fly ash from city refuse incinerator facility and heavy metal sludge with cement additives," *Environmental Science and Pollution Research*, vol. 24, no. 2, pp. 1748–1756, 2017.

[10] Z. Wang, X. Si-fa, and W. Guo-cai, "Study of early strength and shrinkage properties of cement or lime solidified soil," *Energy Procedia*, vol. 16, pp. 302–306, 2012.

[11] M. MacKay and J. Emery, "Stabilization and solidification of contaminated soils and sludges using cementitious systems:

selected case histories," *Concrete research*, Transportation Research Board, no. 1458, pp. 67–72, Washington, DC, USA, 1994.

[12] A. Cheilas, M. Katsioti, A. Georgiades, O. Malliou, C. Teas, and E. Haniotakis, "Impact of hardening conditions on to stabilized/solidified products of cement-sewage sludge-jarosite/alunite," *Cement and Concrete Composites*, vol. 29, no. 4, pp. 263–269, 2007.

[13] F. Ballesteros, A. A. Manila, A. E. S. Choi, and M. C. Lu, "Electroplating sludge handling by solidification/stabilization process: a comprehensive assessment using kaolinite clay, waste latex paint and calcium chloride cement additives," *Journal of Material Cycles and Waste Management*, vol. 21, no. 6, pp. 1505–1517, 2019.

[14] X. Li, C. He, Y. Lv et al., "Utilization of municipal sewage sludge and waste glass powder in production of lightweight aggregates," *Construction and Building Materials*, vol. 256, Article ID 119413, 2020.

[15] L. F. Pires, O. O. S. Bacchi, and K. Reichardt, "Gamma ray computed tomography to evaluate wetting/drying soil structure changes," *Nuclear Instruments and Methods in Physics Research Section B: Beam Interactions with Materials and Atoms*, vol. 229, no. 3-4, pp. 443–456, 2005.

[16] W. Wang, A. N. Kravchenko, A. J. M. Smucker et al., "Effect of wetting and drying cycles on the spatial variability characteristics of the internal structures of soil aggregates," *" Geophysical Research Abstracts*, vol. 10, 2008.

[17] H. M. Jennings, "A model for the microstructure of calcium silicate hydrate in cement paste," *Cement and Concrete Research*, vol. 30, no. 1, pp. 101–116, 2000.

[18] M. M. Allam and A. Sridharan, "Effect of wetting and drying on shear strength," *Journal of the Soil Mechanics and Foundations Division*, vol. 107, no. 4, pp. 421–438, 1981.

[19] Y. Qi, Z. Wang, H. Xu, and Z. Yuan, "Instability analysis of a low-angle low-expansive soil slope under seasonal wet-dry cycles and river-level variations," *Advances in Civil Engineering*, vol. 202012 pages, Article ID 3479575, 2020.

[20] G. S. Guan, H. Rahardjo, and L. E. Choon, "Shear strength equations for unsaturated soil under drying and wetting," *Journal of Geotechnical and Geoenvironmental Engineering*, vol. 136, no. 4, pp. 594–606, 2010.

[21] J. Xu and Y. Ni, "Prediction of grey-catastrophe destabilization time of a granite residual soil slope under rainfall," *Bulletin of Engineering Geology and the Environment*, vol. 78, no. 8, pp. 5687–5693, 2019.

[22] A. W. Yang, Y. Hu, T. Wang et al., "Sludge curing agent and its application, sludge solidified soil," Patent CN106277663A, Tianjin, China, 2017.

[23] Z. J. Chen, "One-dimensional problem with consolidation and time efficiency," *China Civil Engineering Journal*, vol. 5, no. 1, pp. 1–10, 1958.

[24] H. Dob, S. Messast, M. Boulon, and E. Flavigny, "Treatment of the high number of cycles as a pseudo-cyclic creep by analogy with the soft soil creep model," *Geotechnical and Geological Engineering*, vol. 34, no. 6, pp. 1985–1993, 2016.